10-21-2014

LLW-3-6 and Celecoxib Impacts Growth in Prostate Cancer Cells and Subcellular Localization of COX-2

Tokunbo Yerokun
Department of Biology, Spelman College

Leyte L. Winfield
Department of Chemistry and Biochemistry, Spelman College

Published in final edited form as:
Anticancer Res. 2014 September ; 34(9): 4755–4759.

LLW-3-6 and Celecoxib Impacts Growth in Prostate Cancer Cells and Subcellular Localization of COX-2

TOKUNBO YEROKUN[1] and **LEYTE L. WINFIELD**[2]

[1]Department of Biology, Spelman College, Atlanta, GA, U.S.A

[2]Department of Chemistry & Biochemistry, Spelman College, Atlanta, GA, U.S.A

Abstract

The proliferation in human prostate carcinomas, PC3 and MDA-PCa-2b, was analyzed for cells treated with LLW-3-6 and celecoxib in the presence and absence of sulfasalazine. LLW-3-6 was more potent than celecoxib at mediating a dose-dependent reduction of viable PC3 cells. Co-treatment with a non-lethal dose of sulfasalazine diminished the potency of both drugs in this cell line. The effects of the drugs in MDA-PCa-2b cells were less significant than those observed in the PC3 cells. Localization of COX-2 in LLW-3-6- and CBX-treated PC3 cells is consistent with protein aggregation known for cells responding to stress stimuli. To complement this, an analysis of the theoretical binding interactions of LLW-3-6 was completed to illustrate the potential of LLW-3-6 to bind to COX-2 in a manner similar to that of celecoxib. Studies to further define the mechanism of action for LLW-3-6 are ongoing.

Keywords

Benzimidazole; celecoxib; COX-2; sulfasalazine; PC3; MDA-PCa 2b; prostate cancer; docking; focal adhesion

For inflammation-associated human cancers; including those arising from the colon, prostate, brain and lung; the ability of celecoxib (CBX) (Figure 1) to inhibit the enzymatic activity of cyclooxygenase-2 (COX-2) makes te drug an attractive therapeutic option. CBX is reported to prevent the development and progression of a range of cancers. For patients with less severe basal cell carcinoma (BCC), the topical application of CBX is reported to decrease the development of new BCCs by approximately 50% (1). The drug has shown promise as an adjunct to surgery in reducing the number of adenomatous colorectal polyps in patients with hereditary colon cancer susceptibility syndrome such as familial adenomatous polyposis (FAP) and sporadic adenomas (2–4). In addition, CBX has demonstrated anticancer effects in established invasive lung carcinomas and breast cancers, both *in vitro* and *in vivo* (5–7). The use of CBX with other drugs as an adjuvant or neo-adjuvant produced anticancer effects in established invasive lung carcinoma and breast cancer (5, 6, 8) as well. CBX has been reported to inhibit the proliferation of prostate cancer cells; however, this effect has not been reported in prostate cancer patients (9, 10).

Correspondence to: Leyte L. Winfield, Department of Chemistry & Biochemistry, Spelman College, 350 Spelman Lane, SW, Atlanta, Georgia 30314, U.S.A. Tel: +1 4042705748, Fax: +1 4042705752, lwinfield@spelman.edu.

Like CBX, sulfasalazine (SAS) (Figure 1) is of interest for developing combination therapies (11). The clinically approved drug inhibits Akt signaling and cystine-glutamate antiporter system xCT in prostate cancers (12, 13). Its therapeutic effect derives from its metabolite 5-aminosalicylic acid (5-ASA), which acts against ulcerative colitis and other inflammatory diseases. In the prostate cancer cell line DU-145 *in vitro* and PC3 xenografts in nude mice, SAS-induced cystine starvation is reported to inhibit cell growth (14). However, the potential for drug-drug interaction, when used in combination therapy, may antagonize rather than potentiate therapeutic efficacy.

The benzimidazole-based molecule, LLW-3-6 (Figure 1) has not been studied as extensively as its parent compound CBX. The molecule was designed to be structurally similar to CBX, retaining the relative size and shape of CBX while having a reduced lipophilicity with respect to the COX-2 inhibitor. As such, it is expected that the activity of LLW-3-6 would parallel that of CBX. In previous studies, the molecule was reported to inhibit the growth of PC3 cells (15). The present study seeks to further evaluate the activity of LLW-3-6 in comparison to that of CBX. The effects on the proliferation of human prostate carcinoma (PC3 and MDA-PCa-2b) were examined for cells treated with each drug independently and in combination with SAS. PC3 cells, a metastatic adenocarcinoma, are typically used to study the therapeutic utility of drugs against androgen-independent prostate cancers. In comparison, MDA-PCa-2b cells can be utilized to measure drug efficacy in androgen-dependent cells. The proliferation assays were complemented by evaluating the localization of COX-2 after drug treatment and the development of a theoretical model for the interaction of LLW-3-6 with COX-2.

Materials and Methods

Drugs

Celecoxib (CDX, 4-[5-(4-methylphenyl)-3-(trifluoromethyl)-1H-pyrazol-1-yl] benzenesulfonamide) and sulfasalazine (SAS, (E)-2-hydroxy-5-((4-(N-(pyridin-2-yl)sulfamoyl)phenyl)diazenyl) benzoic acid) were purchased from Sigma Chemical Co. (St. Louis, MO, USA). LLW-3-6 (4-(1-(p-tolyl)-1H-benzo[d]imidazol-2-yl)benzenesulfonamide) was synthesized in the lab of Dr. Winfield at Spelman College (15).

Cell culture

The human cancer cell lines were obtained from the American Type Culture Collection (Manassas, VA, USA). Cells were grown in Dulbecco's Modified Eagle's Media (DMEM)/ F12-K culture medium supplemented with 10% fetal bovine serum (FBS), 100-U/ml penicillin and 100-μg/ml streptomycin, maintained at 37°C in a humidified atmosphere of 5% CO_2. Cells were passaged by exposure to trypsin/EDTA and plated at densities of 5×10^5 cells *per* 25-mm culture flask.

Assessment of cell viability

Cells growing near confluency were harvested and re-suspended in culture medium with supplements. The cells were seeded into 96-well plates at 5×10^4 cells *per* well and incubated overnight to allow adhesion and acclimatization. Cells were then rinsed with 1X PBS and

then re-suspended in serum-free F12/DMEM medium. After 2 h, the medium was removed and replaced with fresh medium containing the treatment drug at concentrations of 5, 10, 20 and 40-μM. For co-treated cells, the medium contained the treatment drug at the established concentrations (5, 10, 20 and 40-μM) and 10-μM of SAS. Treatment was terminated by removing the medium containing the drug and adding the cell proliferation WST-1 reagent (Roche Diagnostics, Indianapolis, IN, USA) at 10-fold dilution according to the manufacturer's guidelines. Metabolic cleavage of the WST-1 reagent in cells is accompanied by a change in color from light red to dark red. The intensity of the color directly correlates with the number of metabolically active cells in the culture and was quantified at a wavelength of 450-nm using scanning multi-well spectrophotometer (Midland Scientific Inc., Omaha, NE, USA). Cell viability was reported as percentage of the controls and computed as follows:

$$\%\,\text{viable cells} = \frac{\text{Absorbance } 450-\text{nm (sample)}}{\text{Absorbance } 450-\text{nm (untreated cells)}}$$

All experiments were done in triplicate. Cell viability data are shown as the mean±SEM (Standard Error of Mean) computed from raw data.

Confocal microscopy

Cells on culture slides were fixed with 3% formaldehyde, rinsed with phosphate buffered saline and incubated with a Monoclonal Anti-COX II antibody (Sigma Chemical Co, St. Louis, MO, USA) which was diluted 500-fold in 1% serum. Antibody binding was followed by green fluorescent Alexafluor-conjugated secondary antibody (Invitrogen, Grand Island, NY, USA). The Zeiss 700 Confocal Microscope (Zeiss Company, Germany) was used for visualization. Images were pseudo-colored for contrast with the confocal microscopy, to generate the fluorescent images. Images represent the localization patterns seen with un-treated and treated cells at 40× magnification.

Docking analysis

The structural file for COX-2 in complex with CBX (PDB code: 3LN1) were obtained from the Research Collaboratory for Structural Bioinformatics Protein Data Bank (PDB, http://www.rcsb.org/pdb/home/home.do). Docking models were generated using the Molecular Operating Environment software (Chemical Computing Group, http://www.chemcomp.com/). With the exception of adding protons and optimizing the orientation of groups using the LigX function, all computational analysis are based on data imported from the PDB (16). The best scored structural alignment of LLW-3-6 with CBX was identified and docked into the ligand binding pocket of the COX-2 receptor. The stability of the complex was determined by calculated the energy of the ligand interactions (binding energy) and the overall potential energy of the complex. The energies were calculated using standard parameters defined by Merck Molecular Force Field (MMFF94). Structures with root-mean square deviation (RMSD) close to zero are believe to have a predicted conformation close to that of the original structure.

Results

The dose-dependent pattern for LLW-3-6 toxicity on PC3 cells (Figure 2a) is comparable to the results of previous studies (15). In the former assay, each well contained 500 cells while in the present study 50,000 cells *per* well were used. Although the two-dimensional environment of cells in culture is a far cry from the 3-dimensional microenvironment of a tumor *in vivo*, the use of 50,000 cells *per* well in the assays of the current study is at a cell density similar to that of an *in vivo* tumor mass. The outcomes of the assays show that less than 60% of PC3 cells are viable after treatment with 10- and 20-μM of LLW-3-6 for 48 h, Figure 2a. This is an improved cytotoxic effect over that of CBX for which PC3 cell viability ranged from 65–80% at the same treatment time and concentrations. In comparison to the cytotoxicities of the molecules in PC3 cells, the results in MDA-PCa-2b cells were less favorable. After 24 h of treatment with 20 μM of LLW-3-6, there was approximately a 25% decrease in the number of viable MDA-PCa-2b cells (Figure 2b). However, CBX demonstrates a slight stimulatory effect at this concentration during the first 24 h. At 48 h, the molecules have parallel cytotoxicities in MDA-PCa-2b cells, with CBX being more effective in reducing cell viability.

A non-lethal dose of SAS (10-μM) was used to evaluate the effects of the drug on prostate cell viability when administered with CBX and LLW-3-6. At the maximum concentration tested in combination with SAS, CBX reduced the viability of PC3 cells more than 50%, Figure 2C. In the presence of SAS, treatment with the maximum concentration of LLW-3-6 only reduced cell viability by 20%.

The comparative analysis, Figure 2C, of PC3 cells treated with each drug in presence and absence of SAS suggests SAS antagonizes the activity of LLW-3-6. For both molecules, the combination with SAS resulted in less than 20% cell death in MDA-PCa-2b cells after 48 hours of treatment with 40-μM of the drug (Figure 2d). However, there appears to be a slight improvement in cell treatment outcomes for LLW-3-6 when given in combination with SAS in comparison to the effect of benzimidazole when administered alone.

The localization of COX-2 observed in CBX treated PC3 cells (Figure 3) has not been previously reported, but is consistent with the localization of stress response proteins such as paxillin and vinculin in cells responding to diverse environmental stress stimuli (17). Similarly, the punctuate staining mediated by LLW-3-6 for COX-2 in PC3 cells (Figure 3) is similar to that associated with protein aggregation in cells responding to environmental stress stimuli (18, 19). Due to the limited efficacy of the molecules in the MDA-PCa-2b cells, focal adhesion was not evaluated in this cell line.

Docking analysis was conducted to complement the focal adhesions assays. The results indicate that LLW-3-6 occupy a similar binding orientation to that of CBX (Figure 4). Like CBX, LLW-3-6 forms key hydrogen bonding interactions with Ile503, Gln178 and Ser339. The affinities of the molecule are similar. However, the CBX–COX-2 complex is slightly more stable than that involving LLW-3-6 (potential energy are −5.495 and −2.971 kcal/mol, respectively).

Discussion

In this present study, both LLW-3-6 and CBX was shown to reduce the growth of PC3 cells in a dose- and time-dependent manner. Likewise, both molecules cause COX-2 aggregation in PC3 cells that was indicative of a response to stress stimuli. Drug-drug interaction can affect the therapeutic efficacy of of a molecule. Although it appears that the combined effect of CBX/SAS and LLW-3-6/SAS in PC3 cells are antagonistic, it has not been confirmed if interactions between LLW-3-6 and SAS are responsible for the attenuation of the cytotoxic effects observed for LLW-3-6 in PC3 cells when the molecule was co-administered with SAS. However, the combined effects of these molecules in MDA-PCa-2b, although minimal, appear to enhance the activity of the drugs. The observations of the current report warrant further assessment of LLW-3-6 as a therapeutic option to CBX for tissue-specific cancer treatment as a single drug, but caution needs to be taken with regards to its use in combination drug treatment.

Acknowledgments

The work is funded in part by the National Center on Minority Health and Health Disparities Grant# 5P20MD000215-05 and the National Science Foundation Historically Black Colleges and Universities Undergraduate Program Grant# 0714553. The content is solely the responsibility of the authors and does not necessarily represent the official views of the funding agencies listed.

References

1. Tang JY, Aszterbaum M, Athar M, Barsanti F, Cappola C, Estevez N, Hebert J, Hwang J, Khaimskiy Y, Kim A, Lu Y, So PL, Tang XW, Kohn MA, McCulloch CE, Kopelovich L, Bickers DR, Epstein EH. Basal Cell Carcinoma Chemoprevention with Nonsteroidal Anti-inflammatory Drugs in Genetically Predisposed PTCH1(+/−) Humans and Mice. Cancer Prev Res. 2010; 3:25–34.
2. Arber N, Eagle CJ, Spicak J, Racz I, Dite P, Hajer J, Zavoral M, Lechuga MJ, Gerletti P, Tang J, Rosenstein RB, Macdonald K, Bhadra P, Fowler R, Wittes J, Zauber AG, Solomon SD, Levin B. Celecoxib for the prevention of colorectal adenomatous polyps. New Engl J Med. 2006; 355:885–895. [PubMed: 16943401]
3. Davies NM, McLachlan AJ, Day RO, Williams KM. Clinical pharmacokinetics and pharmacodynamics of celecoxib – A selective cyclo-oxygenase-2 inhibitor. Clin Pharmacokinet. 2000; 38:225–242. [PubMed: 10749518]
4. Zhu JX, Huang JW, Tseng PH, Yang YT, Fowble J, Shiau CW, Shaw YJ, Kulp SK, Chen CS. From the cyclooxygenase-2 inhibitor celecoxib to a novel class of 3-pliosphoinositide-dependent protein kinase-1 inhibitors. Cancer Res. 2004; 64:4309–4318. [PubMed: 15205346]
5. Mao JT, Roth MD, Fishbein MC, Aberle DR, Zhang ZF, Rao JY, Tashkin DP, Goodglick L, Holmes EC, Cameron RB, Dubinett SM, Elashoff R, Szabo E, Elashoff D. Lung Cancer Chemoprevention with Celecoxib in Former Smokers. Cancer Prev Res. 2011; 4:984–993.
6. Miller TW, Rexer BN, Garrett JT, Arteaga CL. Mutations in the phosphatidylinositol 3-kinase pathway: role in tumor progression and therapeutic implications in breast cancer. Breast Cancer Res. 2011; 13
7. Perroud HA, Rico MJ, Alasino CM, Queralt F, Mainetti LE, Pezzotto SM, Rozados VR, Scharovsky OG. Safety and therapeutic effect of metronomic chemotherapy with cyclophosphamide and celecoxib in advanced breast cancer patients. Future Oncol. 2013; 9:451–462. [PubMed: 23469980]
8. Hsu AL, Ching TT, Wang DS, Song XQ, Rangnekar VM, Chen CS. The cyclooxygenase-2 inhibitor celecoxib induces apoptosis by blocking Akt activation in human prostate cancer cells independently of Bcl-2. J Biol Chem. 2000; 275:11397–11403. [PubMed: 10753955]
9. Katkoori VR, Manne K, Vital-Reyes VS, Rodriguez-Burford C, Shanmugam C, Sthanam M, Manne U, Chatla C, Abdulkadir SA, Grizzle WE. Selective COX-2 inhibitor (celecoxib) decreases cellular

growth in prostate cancer cell lines independent of p53. Biotech Histochem. 2013; 88:38–46. [PubMed: 23167625]

10. James ND, Sydes MR, Mason MD, Clarke NW, Anderson J, Dearnaley DP, Dwyer J, Jovic G, Ritchie AWS, Russell JM, Sanders K, Thalmann GN, Bertelli G, Birtle AJ, O'Sullivan JM, Protheroe A, Sheehan D, Srihari N, Parmar MKB, Investigators S. Celecoxib plus hormone therapy versus hormone therapy alone for hormone-sensitive prostate cancer: first results from the STAMPEDE multiarm, multistage, randomised controlled trial. Lancet Oncol. 2012; 13:549–558. [PubMed: 22452894]
11. Lo M, Wang YZ, Gout PW. The x(c)(–) cystine/glutamate antiporter: A potential target for therapy of cancer and other diseases. J Cell Physiol. 2008; 215:593–602. [PubMed: 18181196]
12. Gout PW, Buckley AR, Simms CR, Bruchovsky N. Sulfasalazine, a potent suppressor of lymphoma growth by inhibition of the x(c)(–) cystine transporter: a new action for an old drug. Leukemia. 2001; 15:1633–1640. [PubMed: 11587223]
13. de Groot J, Sontheimer H. Glutamate and the Biology of Gliomas. Glia. 2011; 59:1181–1189. [PubMed: 21192095]
14. Doxsee DW, Gout PW, Kurita T, Lo M, Buckley AR, Wang YW, Xue H, Karp CM, Cutz JC, Cunha GR, Wang YZ. Sulfasalazine-induced cystine starvation: Potential use for prostate cancer therapy. Prostate. 2007; 67:162–171. [PubMed: 17075799]
15. Winfield LL, Smith DM, Halemano K, Leggett CS. A preliminary assessment of the structure-activity relationship of benzimidazole-based anti-proliferative agents. Lett Drug Des Discov. 2008; 5:369–376.
16. Labute, P. Protonate 3D: Assignment of Macromolecular Protonation State and Geometry. Chemical Computing Group Inc; 2007.
17. Turner CE. Paxillin interactions. J Cell Sci. 2000; 113:4139–4140. [PubMed: 11069756]
18. Bunt G, deWit J, vandenBosch H, Verkleij AJ, Boonstra J. Ultrastructural localization of cPLA(2) in unstimulated and EGF/A23187-stimulated fibroblasts. J Cell Sci. 1997; 110:2449–2459. [PubMed: 9410883]
19. Alegre-Abarrategui J, Ansorge O, Esiri M, Wade-Martins R. LRRK2 is a component of granular alpha-synuclein pathology in the brainstem of Parkinson's disease. Neuropath Appl Neuro. 2008; 34:272–283.

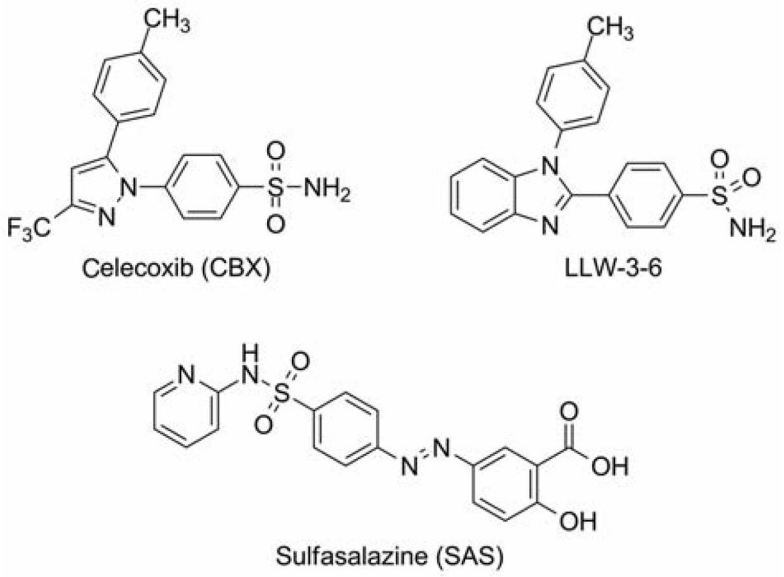

Figure 1.
Drugs.

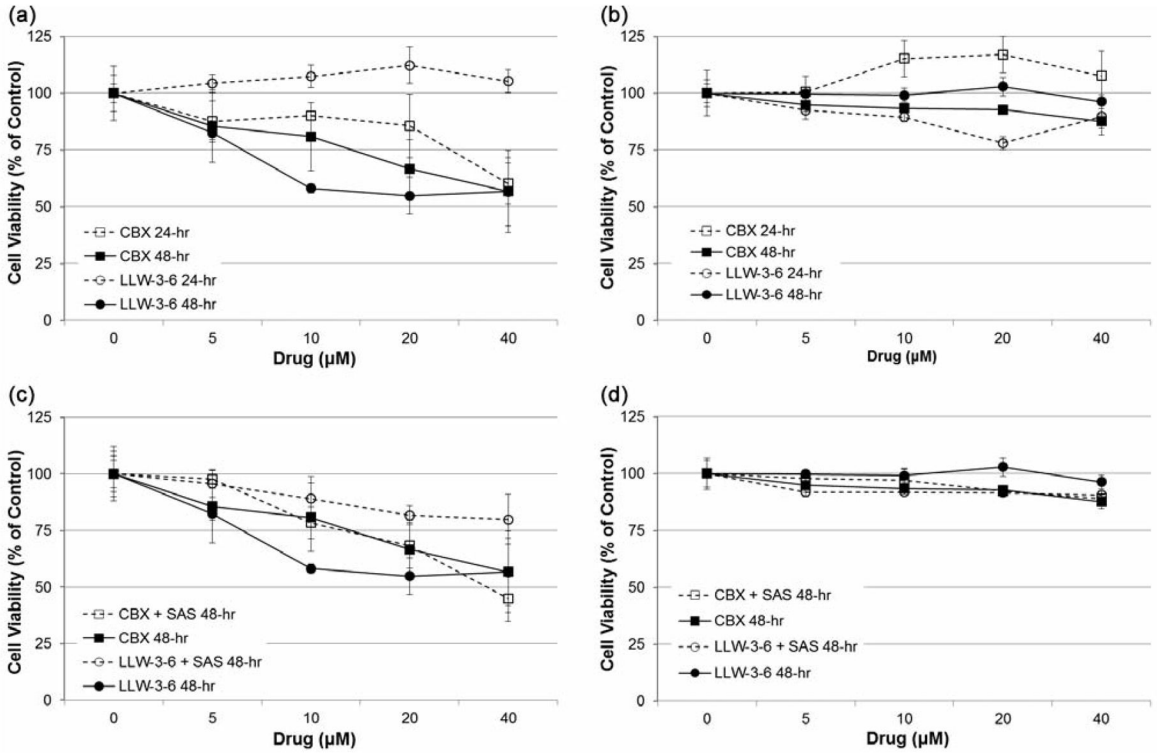

Figure 2.

Viability of prostate cancer cells treated with CBX and LLW-3-6. A modified MTT assay was used to measure cell survival as described in the Materials and Methods section. Bar lines are based on standard error of mean computed for each treatment point. Viability was measured after 24 and 48 h treatments with each drug. (a) Viability of PC3 in the presence of each drug. (b) Viability of MDA-PCa-2b cells in the presence of each drug. (c) Viability of PC3 in presence of each drug and 10-μM of SAS. (d) Viability of MDA-PCa-2b in presence of each drug and 10-μM of SAS.

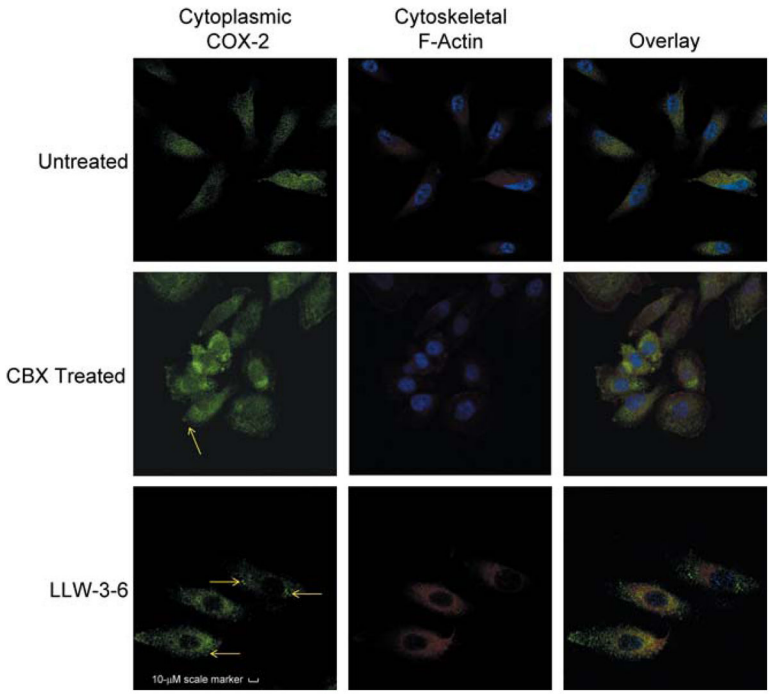

Figure 3.

Localization of COX-2 in PC3 cells. Diffuse fluorescent stain is seen for COX-2 (green) in untreated, CBX-treated, and LLW-3-6-treated PC3 cells. Nuclear stain is in blue. Cytoskeleton was stained for F-actin and is shown in red. COX-2 is found at focal adhesions in CBX treated cells (middle row, yellow arrow). COX-2 punctuate staining in LLW-3-6-treated cells (bottom row, yellow arrow).

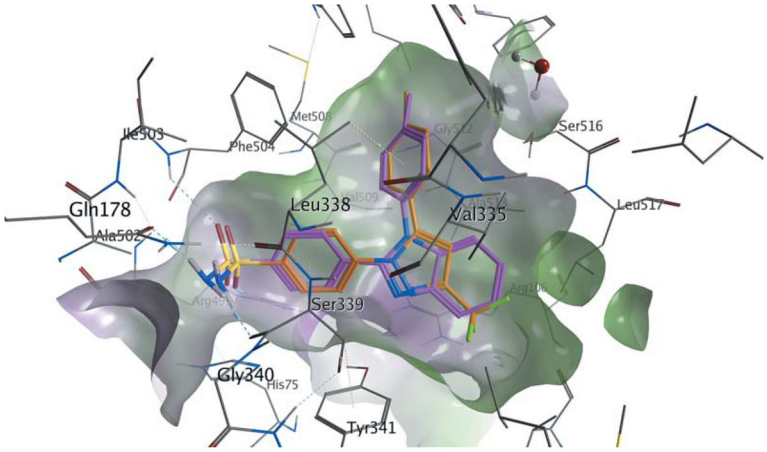

Figure 4.

Model of CBX and LLW-3-6 in the ligand binding pocket of COX-2. CBX is shown in orange tube structure (RMSD=0.165 Å). The calculated binding energy is −9.36-kcal/mol and the overall energy of the complex is −5.495-kcal/mol. LLW-3-6 is shown in pink tube structure (RMSD=0.328 Å). The calculated binding energy is −9.07-kcal/mol and the overall energy of the complex is −2.97-kcal/mol. The residues of COX-2 are shown as grey stick structures with the polar surface of the binding pocket highlighted in pink (hydrophilic) and green (hydrophobic).